Title: Super-resolution track-density imaging studies of mouse brain: comparison to histology

Authors: Fernando Calamante,[a,b], Jacques-Donald Tournier[a,b], Nyoman D. Kurniawan[c], Zhengyi Yang[c], Erika Gyengesi[d], Graham J. Galloway[c], David C. Reutens[c], Alan Connelly [a,b]

Author affiliations:

[a] Brain Research Institute, Florey Neuroscience Institutes, Heidelberg, Victoria, Australia

[b] Department of Medicine, Austin Hospital, University of Melbourne, Melbourne, Victoria, Australia.

[c] Centre for Advanced Imaging, The University of Queensland, Brisbane, Queensland, Australia.

[d] Neuroscience Research Australia, Randwick, New South Wales, Australia.

Corresponding author: Fernando Calamante, Brain Research Institute, Florey Neuroscience Institutes, Melbourne Brain Centre, 245 Burgundy Street, Heidelberg, Victoria 3084, Australia, Phone: (+61 3) 9035 7041, Fax: (+61 3) 9035 7307, Email: fercala@brain.org.au

ABSTRACT

The recently proposed track-density imaging (TDI) technique was introduced as a means to achieve super-resolution using diffusion MRI. This technique is able to increase the spatial resolution of the reconstructed images beyond the acquired MRI resolution by incorporating information from whole-brain fibre-tracking results. It not only achieves super-resolution, but also provides very high anatomical contrast with a new MRI contrast mechanism. However, the anatomical information-content of this novel contrast mechanism has not yet been validated. In this work, we perform such a study using diffusion MRI of *ex vivo* mouse brains acquired at 16.4T, and compare the results of the super-resolution TDI technique to histological staining (myelin and Nissl bodies) in the same brains. Furthermore, a modified version of the directionally-encoded colour TDI map is introduced, which reduces the TDI intensity dynamic range, and therefore enhance the directionality colour-contrast. Good agreement was observed between structures visualised in the super-resolution TDI maps and in the histological sections, supporting the anatomical information-content of the images generated using the TDI technique. The results therefore show that the TDI methodology does provide meaningful and rich anatomical contrast, in addition to achieving super-resolution. Furthermore, this study is the first to show the application of TDI to mouse brain imaging: the high-resolution, high-quality images demonstrate the useful complementary information that can be achieved using super-resolution TDI.

Keywords: magnetic resonance imaging, super-resolution, mouse brain, diffusion MRI, validation, histology

ABBREVIATIONS

3D: three-dimensional;

aca: anterior commissure, anterior part

acp: anterior commissure, posterior part

Br: Bregma;

cc: corpus callosum

cg: cingulum

cp: cerebral peduncle

CSD: constrained spherical deconvolution;

DEC: directionally-encoded colour;

δ: duration of the diffusion-weighted gradient pulse;

Δ: time-interval between the onset of the two gradient pulses;

dhc: dorsal hippocampal commisure

eml: external medullary lamina

f: fornix

FA: fractional anisotropy;

fi: fimbria of the hippocampus

fmi: forceps minor of the corpus callosum

FOD: fibre orientation distributions;

gcc: genu of the corpus callosum

hbc: habenular commisure

ic: internal capsule

iFOD2: 2nd order integration over fibre orientation distributions;

lmax: maximum harmonic order;

lo: lateral olfactory tract

mfb: medial forebrain bundle

ml: medial lemniscus

mt: mammillothalamic tract

ns: nigrostriatal tract

opt: optic tract

pf: precommissural fornix

RGB: red-green-blue;

sm: stria medullaris

st: stria terminalis

*st*TDI: short-tracks track density imaging;

TDI: track density imaging;

TE: echo-time;

TR: repetition-time.
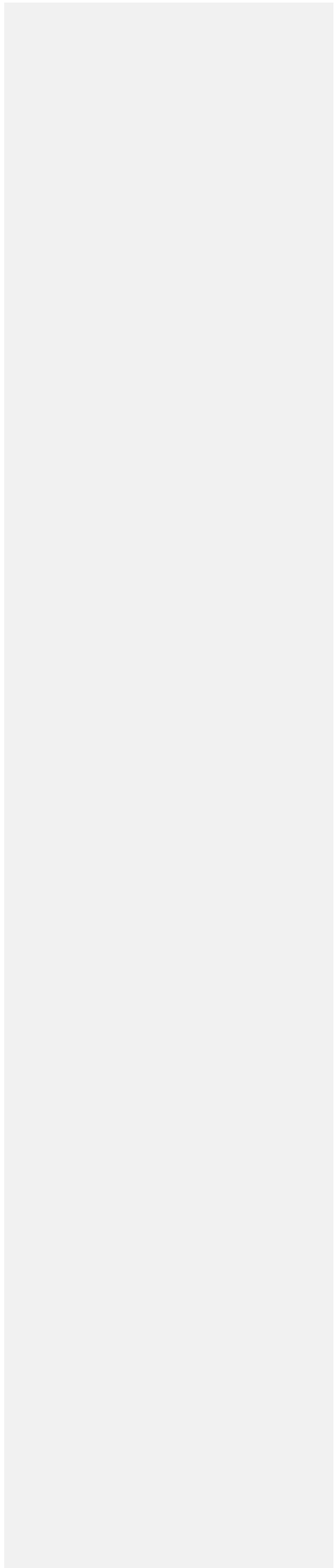
INTRODUCTION

A new method to achieve super-resolution using diffusion MRI has been recently introduced (Calamante et al., 2010). This technique, so-called super-resolution track-density imaging (TDI), is able to increase the spatial resolution of the reconstructed images beyond the acquired MRI resolution by incorporating information contained in whole-brain fibre-tracking results. For example, from 2.5 million tracks obtained using probabilistic fibre-tracking, human brain TDI maps with 125 μm isotropic resolution were created from diffusion MRI data acquired with 2.3 mm resolution on a 3 Tesla standard clinical scanner (Calamante et al., 2010), i.e. a reduction of ~6000 times in the voxel size. More recently, the super-resolution property of the TDI method was validated (Calamante et al., 2011), using both *in vivo* high-resolution human diffusion MRI data acquired at 7 Tesla, and *in silico* diffusion MRI data from a well-characterised numerical phantom (Close et al., 2009). In that study, it was shown that the structures that could be identified in the TDI maps only after using super-resolution were consistent with the corresponding structures identified in the reference high-resolution maps without super-resolution (Calamante et al., 2011).

The TDI technique not only provides a means to achieve super-resolution, but it also provides very high anatomical contrast, with a new MRI contrast mechanism not available from other MRI modalities (Calamante et al., 2010). However, the *anatomical information-content* of this novel contrast mechanism has not yet been validated. It remains to be shown whether the features identified on TDI maps correspond to real brain structures; this requires comparison of the TDI maps with an *anatomical* gold-standard, such as that obtained from histological staining of brain sections.

This study aims to fill this gap, by investigating the anatomical information-content of the TDI technique. Diffusion MRI of *ex vivo* mouse brains were acquired at ultra-high magnetic field strength (16.4 Tesla), and the results of the super-resolution TDI technique were compared to histological staining of the same brains, using myelin stain and Nissl stain (for cell bodies).

MATERIALS AND METHODS

Three 12-week old adult C57 BL6 mice (*m1*, *m2* and *m3*) were included in this study. Mice were anaesthetised and perfused with 4% paraformaldehyde containing 0.5% Magnevist. The brains were removed from the skull and placed in Fomblin for MRI. All mice were housed and handled in accordance with … *Brief description to be completed by Nyoman or somebody else from UQ* …

MRI data acquisition

Diffusion MRI data were acquired using previously published protocols (Moldrich et al., 2010). In brief, MRI data were acquired on a 16.4 Tesla vertical bore animal system (Bruker Biospin, Germany) using a 15 mm linear surface coil (M2M, Australia). The diffusion acquisition consisted of a 3D diffusion-weighted spin-echo sequence, with TE/TR= 22.8/400 ms, 0.1 mm isotropic resolution, two b=0 s/mm^2 images and 30 uniformly distributed diffusion gradient-encoding directions (Jones et al., 1999) with b=5000 s/mm^2 (δ/Δ=2.5/14 ms). The total acquisition time was ~32 hours.

Fibre-tracking

Mouse whole-brain fibre-tracking was carried out using in-house software based on *MRtrix* (Brain Research Institute, Melbourne, Australia, http://www.brain.org.au/software/). The analysis included constrained spherical deconvolution (CSD) (Tournier et al., 2007) to model multiple fibre orientations in each voxel, with a maximum harmonic order $l_{max} = 6$; this parameter determines the 'sharpness' of the fibre orientation distributions (Tournier et al., 2004; Tournier et al., 2008). Probabilistic fibre-tracking (Behrens et al., 2003) was performed using the 2nd order integration over fibre orientation distributions (iFOD2) algorithm (Tournier et al., 2010); this included the following relevant parameters: 0.1 mm step-size, maximum angle between steps = 45º, three FOD samples/step, any track with length < 0.4 mm was discarded, termination criteria: exit the brain or when the CSD fibre-orientation distribution amplitude was < 0.01 (Note: this FOD cut-off value was reduced compared with that used for *in vivo* human brain studies (Tournier et al., 2010,

Calamante et al., 2011), and was empirically chosen based on a preliminary assessment of tracking in one of the *ex vivo* mouse brains). To achieve whole-brain tracking, random seeds were placed throughout the mouse brain, and tracking was performed bi-directionally. A total of 4,000,000 tracks were generated for each mouse data-set.

Track-density Imaging (TDI)

TDI maps were generated using *MRtrix* by calculating the total number of tracks present in each element of a grid. By selecting a grid-element smaller than the voxel size of the source data, the spatial resolution of the final map can be increased, thus achieving super-resolution (see Calamante et al. (2010) for further details). For each mouse dataset, a 20 μm isotropic grid was used to generate the super-resolution TDI map; this corresponds to a 125-fold reduction in the voxel size, compared to the acquired resolution.

Modified directionally-encoded colour (DEC) TDI

A directionally-encoded colour (DEC) version of the TDI maps was proposed in (Calamante et al., 2010) as the super-resolution equivalent of the conventional DEC map in diffusion tensor imaging. One limitation of these super-resolution DEC maps is that the increased dynamic range of the TDI map (as compared with that of the fractional anisotropy map used in the diffusion tensor case (Pajevic and Pierpaoli, 1999)) compromises the visual appearance of low-intensity structures in the TDI map. This is particularly the case in the mouse brain, where the major white matter structures (e.g. the corpus callosum) have a relatively much larger signal intensity in the TDI map (e.g. see Fig. 2 below). To overcome this limitation, a modified version of the DEC TDI maps was created by *constraining* the maximum length of each track to 1 mm (NB. since this length corresponds to 10 acquired voxels, sufficient medium-range fibre-tracking information is retained to allow the super-resolution step to introduce meaningful intra-voxel information). The resulting DEC TDI map will be referred to as *DEC short-tracks TDI (stTDI)* map. By constraining the length of the tracks, the contribution of each seed-point within a long white matter bundle (e.g. corpus callosum) only contributes to the TDI values within a 1 mm neighbourhood, thus reducing the TDI contrast.

Importantly, this improves the visual appearance of the colour-contrast in the DEC *st*TDI maps (Note that in the DEC maps the relevant contrast information is contained in the colour, rather than the image intensity). However, since the TDI intensity is greatly reduced overall (each shorter track only contributes intensity to a smaller number of voxels), a much larger number of tracks needs to be generated to maintain a reasonable contrast-to-noise ratio. For this study, 65 million tracks were therefore generated for each mouse brain data-set with the short track constraint, and DEC *st*TDI maps constructed with 20 μm isotropic resolution.

Histology

Histology was performed with myelin staining for the brains of mice *m1* and *m2,* and Nissl stain (cell bodies) for mouse *m3*. … *Brief description of the myelin and Nissl staining procedures from somebody from UQ and/or NSW* …

Image registration

When a sufficient number of histological sections were available, these sections were reconstructed as a 3D stack and registered to the TDI maps. Otherwise, the TDI slices closer to the available histological sections were visually identified. … *Brief description of the 3D stack reconstruction and histology-TDI registration steps to be completed by Steven* …

RESULTS

Fig. 1 shows representative examples of whole-brain fibre-tracking results in the mouse brain. For visualisation purposes, only 100,000 tracks have been displayed. As can be appreciated in the figure, the combination of CSD and iFOD2 tracking produce very high-quality whole-brain fibre-tracking results from these diffusion MRI data.

Fig. 2 shows a typical example of coronal, horizontal and sagittal TDI maps, as well as the corresponding native-resolution fractional anisotropy (FA) maps. The FA maps have been included to illustrate the increase in spatial resolution achieved by super-resolution, as well as to emphasise

the different contrast information present in the TDI maps. The increase in spatial resolution can be further appreciated in the zoomed examples displayed in Fig. 3, where the sharper delineation of the complex structures in the hippocampus and cerebellum is clearly visible in the super-resolution TDI maps.

Fig. 4 shows the corresponding DEC TDI maps, DEC *st*TDI maps and conventional tensor-based DEC maps, with the RGB color-coding indicating the main local orientation. These images illustrate the increased directional information in the DEC *st*TDI maps (cf. DEC TDI maps). Due to their track-length constraint, the DEC *st*TDI maps display good directional information in both long tracts (such as the corpus callosum, the fasciculus retroflexus and the fornix precommissuralis, see yellow, green and orange arrows respectively) and short bundles (such as the commissurae thalami and the tractus solitarius, see white and gray arrows respectively). Furthermore, the DEC *st*TDI maps still retain the super-resolution properties of the TDI method, thus showing increased resolution compared to the conventional DEC maps.

A comparison of the structures visualised in the TDI maps and those identified in myelin staining in the *m1* mouse are shown in Fig. 5 for a representative subset of coronal slices. As can be appreciated in these images, there is a striking correspondence between many of the structures present in both imaging modalities (see figure legend for a list of some of these anatomical structures). Fig. 6 shows equivalent results for the data from the *m2* mouse, enabling a visual comparison between the TDI maps and myelin staining images over a larger extent, from cranial coronal slices to caudal slices including the cerebellum. The visual correspondence between many of the structures across the various coronal levels can be clearly appreciated.

Fig. 7 shows an equivalent comparison for the *m3* mouse, with the corresponding TDI maps and Nissl staining images shown for a representative subset of horizontal slices. Once again, the similarity between many of the structures visualised by both imaging modalities is readily appreciated.

Comment [FC1]:
I have labeled these structures by looking at an atlas. Could please other co-author with more mouse anatomical knowledge confirm this labeling? Thanks.

Comment [FC2]:
Thanks to Erika for her help with this part!

DISCUSSION

We have presented an assessment of the anatomical information-content of the TDI technique by comparing the structures visualised in TDI maps from mouse brains with those identified in histological staining of the same brains. The striking agreement between structures visualised in the super-resolution TDI maps and the myelin and Nissl stained histological sections corroborates the anatomical information-content of the images generated using the TDI technique. The results therefore show that the TDI methodology provides a rich anatomical contrast that is biologically meaningful. The current study therefore is complementary to our previous validation of the super-resolution property of TDI (Calamante et al., 2011).

It should be noted that, since the diffusion MRI contrast mechanism is not B_0-dependent, the biologically meaningful TDI contrast demonstrated in the current study using ultra-high field 16.4T MRI should still be valid for the lower magnetic field strengths more commonly used in experimental and clinical studies. Therefore, the current results also serve to corroborate the anatomical validity of the high-contrast structures demonstrated previously by TDI in human studies at 3T (Calamante et al., 2010).

The comparison between the TDI maps and histological staining in this study was performed in a qualitative manner. A formal quantitative comparison of the agreement between these imaging methodologies is not straightforward due to the different contrast mechanisms. It should be noted that, for the same reason, all of the structures identified in the TDI map are not necessarily expected to have an equivalent in the histological stained images, and vice versa. Furthermore, and more importantly, despite the use of image registration between MRI and histology in two of the mice data-sets (*m2* and *m3*), the presence of residual registration errors is unavoidable.

This study also introduces a variant of the DEC TDI technique, the so-called DEC *st*TDI, which reduces the dynamic range of the intensity of the TDI maps while still retaining the directional information. Therefore, the DEC *st*TDI maps retain high local fibre directional contrast (encoded by the RGB colours), while having the benefit of a more uniform intensity than the DEC TDI maps. By

constraining the maximum length of each track, the DEC stTDI technique does not 'penalise' the DEC contrast in short fibre bundles (cf. DEC TDI maps in Fig. 4). Importantly, since the length constraint is several voxels in length (in our case, 10 acquired voxels), the fibre-tracks still retain medium-range information, and therefore sufficient intra-voxel information to achieve super-resolution. On the other hand, as explained in the Materials and Methods section, the number of tracks required to generate the DEC stTDI maps is approximately an order of magnitude greater. However, since each track is much shorter, the processing-time and track file size are similar.

The use of diffusion MRI fibre-tracking to study mouse brain has been the subject of previous research (e.g. Huang et al., 2004; Moldrich et al., 2010; Harsan et al., 2010; Jiang and Johnson, 2010; Boretius et al., 2009; Chuang et al., 2011). Our work is fundamentally different to these studies in that the tracking was used primarily to generate super-resolution structural images with a novel source of contrast. The main purpose of our study therefore is the validation of such images by direct comparison to histological sections.

Apart from validating the TDI methodology, this study is the first to show the application of this new technique to mouse brain imaging. The high-resolution, high-quality images shown in the current study demonstrate the useful complementary information that can be achieved using super-resolution TDI. Due to the increasing interest in mouse brain mapping and imaging phenotypes in mouse models of neurological disorders (e.g. Wadghiri and Helpern, 2007; Waerzeggers et al., 2010), the TDI methodology should provide a very useful additional imaging modality. Furthermore, this methodology could also play an important role in the study of other animal species, when high-resolution imaging with good white matter contrast is needed.

In conclusion, the good agreement observed between structures visualised in the super-resolution TDI maps and in the histological sections supports the veracity of the anatomical information-content of the images generated using the TDI technique. Therefore, the TDI methodology does provide rich anatomical contrast that is biologically meaningful, in addition to achieving super-resolution.

FIGURE LEGENDS

Fig. 1: Example of whole-brain fibre-tracking results from mouse *m3*. (Top-left) Surface view from a dorso-posterior direction. Coronal section (top-right), sagittal section (bottom-left) and horizontal section (bottom-right) of whole-brain fibre-tracking results; each section displays the tracks within a 0.2 mm slab. The colour-coding indicate the local fibre orientation (red: left-right, green: dorsal-ventral, blue: cranial-caudal). The results correspond to 100,000 tracks.

Fig. 2: Super-resolution TDI maps (left column) and FA maps (right column), for coronal (top), horizontal (middle) and sagittal (bottom) orientations. The TDI maps have 20 μm isotropic resolution; the FA maps have 100 μm resolution (i.e. the resolution of the acquired diffusion-weighted imaging data).

Fig. 3: Zoomed regions of super-resolution TDI maps (middle column) and FA maps (right column). The zoomed region is indicated by the rectangle on the TDI maps shown in the left column). Top row: coronal slice with zoomed region in the hippocampus; bottom row: sagittal slice with zoomed region in the cerebellum. The TDI maps have 20 μm isotropic resolution; the FA maps have 100 μm resolution.

Fig. 4: Directionally-encoded colour (DEC) TDI maps (left column), DEC *st*TDI maps (middle column), and conventional tensor-based DEC maps (right column), for coronal (top), horizontal (middle) and sagittal (bottom) orientations (Note: these slices correspond to the same slices displayed in Fig. 2). The colour-coding indicate the local fibre orientation (for the TDI maps) or the

principal direction of the diffusion tensor (for the tensor-based map). Red: left-right, green: dorsal-ventral, blue: cranial-caudal. The TDI-based DEC maps have 20 μm isotropic resolution; the tensor based DEC maps have 100 μm resolution. The DEC *st*TDI maps display good directionality information in both long and short bundles (e.g. see yellow, green, orange, white and gray arrows for the corpus callosum, the fasciculus retroflexus, the fornix precommissuralis, the commissurae thalami and the tractus solitarius, respectively); some of these structures have very high intensity (and therefore appear 'saturated') in the DEC-TDI maps, or they have very low intensity and are barely seen in these maps.

Fig. 5: Comparison of TDI maps with myelin staining for the brain of mouse *m1*. Example coronal slices (at three different anatomical positions) from myelin staining (top row), super-resolution TDI maps (middle row) and super-resolution DEC *st*TDI maps (bottom row). The colour-coding indicate the local fibre orientation (red: left-right, green: dorsal-ventral, blue: cranial-caudal). The super-resolution maps have 20 μm isotropic resolution. The distance to Bregma for each histological slice is indicated in the figure. Abbreviations: aca – anterior commissure, anterior part; acp – anterior commissure, posterior part; cc – corpus callosum; cg – cingulum; cp – cerebral peduncle; dhc – dorsal hippocampal commisure; eml – external medullary lamina; f – fornix; fi – fimbria of the hippocampus; fmi – forceps minor of the corpus callosum; gcc – genu of the corpus callosum; hbc – habenular commisure; ic – internal capsule; lo – lateral olfactory tract; mfb – medial forebrain bundle; ml – medial lemniscus; mt – mammillothalamic tract; ns – nigrostriatal tract; opt – optic tract; pf – precommissural fornix; sm – stria medullaris; st – stria terminalis.

Fig. 6: Comparison of TDI maps with myelin staining for the brain of mouse *m2*. Example coronal slices (at 10 different levels) from myelin staining (a), super-resolution TDI maps (b) and super-resolution DEC *st*TDI maps (c). The colour-coding indicate the local fibre orientation (red: left-right, green: dorsal-ventral, blue: cranial-caudal). The super-resolution maps have 20 μm isotropic resolution.

Fig. 7: Comparison of TDI maps with Nissl staining for the brain of mouse *m3*. Example horizontal slices (at four different levels) from 3D-reconstructed Nissl staining (top row), super-resolution TDI maps (middle row) and super-resolution DEC *st*TDI maps (bottom row). The colour-coding indicate the local fibre orientation (red: left-right, green: dorsal-ventral, blue: cranial-caudal). The super-resolution maps have 20 μm isotropic resolution.

REFERENCES

Behrens, T.E., Johansen-Berg, H., Woolrich, M.W., Smith, S.M., Wheeler-Kingshott, C.A., Boulby, P.A., Barker, G.J., Sillery, E.L., Sheehan, K., Ciccarelli, O., Thompson, A.J., Brady, J.M., Matthews, P.M., 2003. Non-invasive mapping of connections between human thalamus and cortex using diffusion imaging. *Nature Neurosci*. **6**, 750–757.

Boretius, S., Michaelis, T., Tammer, R., Ashery-Padan, R., Frahm, J., Stoykova, A., 2009. In vivo MRI of altered brain anatomy and fiber connectivity in adult pax6 deficient mice. *Cereb Cortex*. **19**, 2838–2847.

Calamante, F., Tournier, J.-D., Heidemann, R.M., Anwander, A., Jackson, G.D., Connelly, A., 2011. Track density imaging (TDI): validation of super-resolution property. *NeuroImage*; doi:10.1016/j.neuroimage.2011.02.059.

Calamante, F., Tournier, J.-D., Jackson, G.D., Connelly, A., 2010. Track Density Imaging (TDI): Super-resolution white matter imaging using whole-brain track-density mapping. *NeuroImage* **53**, 1233-1243.

Chuang, N., Mori, S., Yamamoto, A., Jiang, H., Ye, X., Xu, X., Richards, L.J., Nathans, J., Miller, M.I., Toga, A.W., Sidman, R.L., Zhang, J., (2011). An MRI-based atlas and database of the developing mouse brain. *Neuroimage* **54**, 80-89.

Close, T.G., Tournier, J.-D., Calamante, F., Johnston, L.A., Mareels, I., Connelly, A., (2009). A software tool to generate simulated white matter structures for the assessment of fibre-tracking algorithms. *NeuroImage* **47**, 1288–1300.

Harsan, L.A., Paul, D., Schnell, S., Kreher, B.W., Hennig, J., Staiger, J.F., von Elverfeldt, D., 2010. In vivo diffusion tensor magnetic resonance imaging and fiber tracking of the mouse brain. *NMR Biomed.* **23**, 884–896.

Huang, H., Zhang, J., van Zijl, P.C., Mori, S., 2004 Analysis of noise effects on DTI-based tractography using the brute-force and multi-ROI approach. *Magn Reson Med.* **52**, 559–565.

Jiang, Y., Johnson, G.A., 2010. Microscopic diffusion tensor imaging of the mouse brain. *NeuroImage* **50**, 465–471.

Jones, D.K., Horsfield, M.A., Simmons, A., 1999. Optimal strategies for measuring diffusion in anisotropic systems by magnetic resonance imaging. *Magn. Reson. Med.***42**, 515–525.

Moldrich, R.X., Pannek, K., Hoch, R., Rubenstein, J.L., Kurniawan, N.D., Richards, L.J., 2010. Comparative mouse brain tractography of diffusion magnetic resonance imaging. *NeuroImage* **51**, 1027–1036.

Pajevic, S., Pierpaoli, C., 1999. Color schemes to represent the orientation of anisotropic tissues from diffusion tensor data: application to white matter fiber tract mapping in the human brain. *Magn Reson Med.* **42**, 526-540.

Tournier, J.D., Calamante, F., Connelly, A., 2007. Robust determination of the fibre orientation distribution in diffusion MRI: non-negativity constrained super-resolved spherical deconvolution. *NeuroImage.* **35**, 1459-1472.

Tournier, J.D., Calamante, F., Connelly, A., 2010. Improved probabilistic streamlines tractography by 2nd order integration over fibre orientation distributions. *In: Proc. 18th Annual Meeting of the Intl. Soc. Mag. Reson. Med. (ISMRM)*, Stockholm, Sweden, 2010; **18**, p.1670.

Tournier, J.D., Calamante, F., Gadian, D.G., Connelly, A., 2004. Direct estimation of the fibre orientation density function from diffusion-weighted MRI data using spherical deconvolution. *NeuroImage.* **23**, 1176–1185.

Tournier, J.D., Yeh, C.H., Calamante, F., Cho, K.H., Connelly, A., Lin, C.P., 2008. Resolving crossing fibres using constrained spherical deconvolution: Validation using diffusion-weighted imaging phantom data. *NeuroImage* **42**: 617–625.

Wadghiri, Y.Z., Helpern, J.A., 2007. MR of transgenic mice. *NMR Biomed.* **20**, 151–153.

Waerzeggers, Y., Monfared, P., Viel, T., Winkeler, A., Jacobs, A.H., 2010. Mouse models in neurological disorders: Applications of non-invasive imaging. *Biochim Biophys Acta* **1802**, 819–839.